Unravelling the structure of chemisorbed CO_2 species in mesoporous aminosilicas: a critical survey

Rui Afonso, Mariana Sardo, Luís Mafra*, José R. B. Gomes*

CICECO – Aveiro Institute of Materials, Department of Chemistry, University of Aveiro, Campus Universitário de Santiago, 3810-193 Aveiro, Portugal

*e-mail addresses: lmafra@ua.pt; jrgomes@ua.pt

Abstract

Chemisorbent materials, based on porous aminosilicas, are amongst the most promising adsorbents for direct air capture applications, one of the key technologies to mitigate carbon emissions. Herein, a critical survey of all reported chemisorbed CO_2 species, which may form in aminosilica surfaces, is performed by revisiting and providing new experimental proofs of assignment of the distinct CO_2 species reported thus far in the literature, highlighting controversial assignments regarding the existence of chemisorbed CO_2 species still under debate. Models of carbamic acid, alkylammonium carbamate with different conformations and hydrogen bonding arrangements were ascertained using density functional theory (DFT) methods, mainly through the comparison of the experimental ^{13}C and ^{15}N NMR chemical shifts with those obtained computationally. CO_2 models with variable number of amines and silanol groups were also evaluated to explain the effect of amine aggregation in CO_2

speciation under confinement. In addition, other less commonly studied chemisorbed CO_2 species (*e.g.*, alkylammonium bicarbonate, ditethered carbamic acid and silylpropylcarbamate), largely due to the difficulty in obtaining spectroscopic identification for those, have also been investigated in great detail. The existence of either neutral or charged (alkylammonium siloxides) amine groups, prior to CO_2 adsorption, is also addressed. This work extends the molecular-level understanding of chemisorbed CO_2 species in amine-oxide hybrid surfaces showing the benefit of integrating spectroscopy and theoretical approaches.

Introduction

Given the negative environmental consequences associated with CO_2 emissions, a great effort has been placed in discovering and developing CO_2 capture solutions, with amine-based solid adsorbents emerging as good sorbent materials [1-4]. This is especially the case for low concentration, low temperature, moisture-containing applications [5-7]. In the case of direct air capture [8], companies like Climeworks [9-10] and Global Thermostat [11-12] are already using solid amine-based sorbents. Some cases of post-combustion CO_2 capture have also been proposed for their application [13-15]. Assessing the type of chemisorbed CO_2 structure formed in such porous amine adsorbents is of paramount importance to design and optimise materials for such applications. A recent review article carefully expands on the relation between structure and performance [16].

Many researchers have tried to better understand the nature of the CO_2 sorption process on these materials. Although it is well established that chemical reactions (chemisorption) occur upon adsorption of CO_2 in amine covered surfaces, the type of

47 species formed, their stability under different conditions, and the variables influencing
48 their relative proportions are still under great debate. Over the last decades, many
49 studies have presented spectroscopic evidence for the different types of CO_2-amine
50 adducts formed, with a plethora of distinct species being proposed, both for
51 alkylamine-grafted [1-2, 17-35] and polyimine-impregnated mesoporous silicas [3-4, 22, 26, 28, 36-
52 38]. The main species identified were ammonium carbamate [1-2, 19, 21, 23-25, 27-31, 33-38],
53 carbamic acid [17-18, 21, 24-25, 28-38] and ammonium bicarbonate [1-2, 17-18, 22, 29, 33-35, 37-38], with
54 urea [22, 24, 27-28] and surface-bonded carbamate (silylpropylcarbamate) [23-24, 29, 37] forming
55 under special conditions.

56 Traditionally, Fourier-transform infrared (FTIR) spectroscopy has been used as the
57 leading tool in species identification. More recently, nuclear magnetic resonance
58 (NMR) has emerged as a powerful alternative [39], able to discriminate not only between
59 different species [25, 27-28, 30, 34-35, 40-46], but also different conformations of the same
60 species [32, 47]. These studies use mainly ^{13}C NMR, in order to detect CO_2-amine
61 adducts. Many authors, including our group, were able to observe two ^{13}C resonances
62 around 160-161 and 164-165 ppm (Table S20), typically attributed to carbamic acid
63 and carbamate ions, respectively, under different experimental conditions and in
64 different materials [25, 27, 30, 32, 40-45, 47]. While carbamic acid formation is typically
65 attributed to isolated amines, and ammonium carbamates to amine pairs, it has been
66 shown experimentally and computationally that it is possible to have either paired or
67 isolated carbamic acid [32, 47]. In addition, an extra peak at 153.3 ppm (Table S20) was
68 observed by our group, which has been attributed to a CO_2 species extremely
69 sensitive to the presence of water, appearing only in absolutely anhydrous conditions.
70 This resonance has been assigned to the presence of isolated amines reacting with
71 CO_2 to form carbamic acid [47].

Pinto et al. [25] were the first to use ^{15}N NMR to analyse surface CO_2-amine adducts, but the low abundance of the isotope leads to results with an extremely low signal-to-noise radio. Recent contributions by Jones and co-workers [34-35] used a two-step synthesis process to enrich the grafted amines in ^{15}N, where 3-bromopropylsilane is first grafted onto the silica pore surface, and later $^{15}NH_3$ is made to react with the grafted chains [48]. By means of ^{15}N cross polarization magic-angle spinning (CPMAS) NMR, three different amine/ammonium species were assigned to the ^{15}N resonances associated to amine (δ_N ~ 24 ppm), ammonium siloxide (δ_N ~ 32 ppm) and ditethered amine (δ_N ~ 44 ppm). The latter species appears as an artefact of the unique synthesis procedure employed. Upon adsorption of CO_2, an additional resonance appeared, at δ_N ~ 88 ppm, which has been assigned to carbamic acid and ammonium carbamate species.

Herein, a critical survey of all reported chemisorbed CO_2 species formed in primary amine-modified mesoporous silicas is made, by performing new solid-state NMR (ssNMR) experiments, assisted by electronic density functional theory (DFT) modelling calculations. Although some of these CO_2 species have been hypothesised in previous studies, they have never been modelled and this work tries to fill this gap. This work confirms and, in some cases, disproves experimental resonance assignments reported in the literature, while revisiting previous DFT models. In addition, new models are provided which explain the formation of CO_2 species under distinct amine aggregation states. Comparison of experimental and theoretical infrared spectra are also consistent with these assignments.

Experimental section

The approach and methods used in the calculations performed in this work were described elsewhere [32, 49]. Sample preparation and NMR measurements were performed according to previously reported experimental conditions [32, 47, 50]. A detailed description of the used methods and techniques is provided in the Supporting Information.

Results and Discussion

The most stable structures (*i.e.*, minima on the potential energy surfaces) of the species modelled in the present work are shown in Figures 1 and S2, and the corresponding ^{15}N and ^{13}C calculated chemical shifts (CSs) are presented in Tables 1 and S1, respectively. Several starting possibilities for carbonaceous species that may form in silica functionalized with primary amines were considered; for a complete set of structural models please refer to Tables S2-14.

Alkylamine and alkylammonium chains

The calculated ^{15}N CS (Table S1) are in very good agreement with the experimental values (RMSD ~ 2.5±1.4 ppm). Overall, there is a systematic but small positive shift in the calculated values compared to the experimental ones. Such cases occasionally occur when using DFT methods to calculate ^{15}N NMR CSs [51-53], and were also observed in the case of the aqueous alkylamines considered here to determine a

reference root-mean-square error (see computational details and calculated values in Table S25).

The clusters used to model amines and ammoniums consider a single amine and a single silanol attached to the silica surface (Figure S2), hence simulating a relatively high amine density but below monolayer coverage. Structural optimisations do not spontaneously lead to the formation of propylammonium siloxide, an *a priori* plausible scenario. Thus, to determine the ^{15}N CS for the ammonium ion, it was necessary to freeze the three N-H lengths at 1.017 Å (typical N-H distance in primary amines and ammonia) during geometry optimisation. This suggests that the adsorbed propylammonium siloxide species (**11**, Figure S2) is far less stable than the co-adsorbed neutral propylamine and silanol groups onto the silica surface (**10**, Figure S2). Indeed, the most stable propylammonium siloxide structure yields a Gibbs free energy of formation 99.6 kJ/mol higher than the most stable neutral amine model (Table S15), which suggests that the former species is very unlikely to form under the conditions assumed in our calculations. This turns out not to be the case in the real system, as discussed further below.

Among all species listed in Table S1, the single-tethered amine (**10,** Figure S2) is the one showing the largest deviation between the calculated and the experimental CS values, 27.9 and 24 ppm, respectively. This minor overestimation is typical for ^{15}N CS determination using DFT methods. However, it is still interesting to notice that this ^{15}N resonance reported by Shimon et al. [35], with lower amine concentrations, is slightly more shielded when compared to those of Chen et al. [34], with higher amine concentration. In fact, amine concentrations in Chen et al. are close to monolayer coverage, so interactions with silanols should be relatively rare. It may thus be that the

single-silanol, single-amine cluster is more suited to represent the systems of Shimon et al. [35] than those of Chen et al. [34], from where the 24 ppm value is originally taken.

The calculated propylammonium ion ^{15}N CS (**11,** Figure S2) is remarkably close to the experimental value (33.1 and 32 ppm, respectively), which supports the original assignment [34]. Although other contributions have previously hypothesised the existence of propylammonium siloxide species [24, 31, 36-37, 54], this is the first computational evidence strongly supporting the presence of this species prior to contact with CO_2. The fact that propylammonium siloxide does not occur spontaneously (and is, indeed, much less favoured than the neutral species) in our model, but seems to occur in the real system, may be ascribed to the simplicity of the model employed. From our experience, complex H-bond networks, involving several electronegative atoms and protons, are necessary to stabilise proton transfer in these species. Charged species are often stabilised by water molecules [55]; indeed, the presence of residual water may be fundamental for the formation of propylammonium cations [34]. Therefore, the formation and stabilization of propylammonium siloxide in the systems studied experimentally can be associated to the presence of either aggregates of silanols and amines at close distance or moisture. The ^{15}N enrichment method used by Jones and co-workers generates a ditethered secondary amine byproduct. The structure model of this species (**12**, Figure S2) exhibits a calculated CS extremely close to the respective experimental value (45.1 vs. 44 ppm, respectively). As hypothesised [34], these species have extremely rigid chains, greatly limiting the number of stable conformations arising from the DFT optimisations.

The analysis above confirms that both amines and ammonium siloxide ion pairs are present in aminated silicas, and that under certain synthesis conditions ditethered amines may form.

Table 1. Experimental and calculated ^{13}C and ^{15}N CSs for different CO_2-amine adducts. Calculated values correspond to the structures shown in Figure 1. Experimental ^{15}C CSs values were taken from the NMR spectra of Figure 2 and from ref. [46] (in the case of ammonium bicarbonate). Experimental ^{15}N CSs were taken from [35].

Label	Species	Calculated	Experimental	SI Tables
1	Ammonium Carbamate	δ_C = 163.7 ppm δ_{N1} = 90.4 ppm δ_{N2} = 34.5 ppm	δ_C = 164.3 ppm δ_{N1} = 88 ppm δ_{N2} = 32 ppm	Table S6 21 Structures
2	Carbamic Acid 2 amines, 1 silanol	δ_C = 159.3 ppm δ_{N1} = 91.2 ppm δ_{N2} = 31.7 ppm	δ_C = 161.3 ppm δ_{N1} = 88 ppm δ_{N2} = 24 ppm	Table S7 25 Structures
3	Carbamic Acid 2 amines, 0 silanol	δ_C = 161.8 ppm δ_{N1} = 92.6 ppm δ_{N2} = 31.7 ppm	δ_C = 161.3 ppm δ_{N1} = 88 ppm δ_{N2} = 24 ppm	Table S8 12 Structures
4	Carbamic Acid 1 amine, 1 silanol	δ_C = 158.2 ppm δ_N = 83.3 ppm	δ_C = 159.5 ppm δ_N = 88 ppm	Table S9 5 Structures
5	Carbamic Acid 1 amine, 5 silanols	δ_C = 156.1 ppm δ_N = 96.2 ppm	δ_C = 153.7 ppm δ_N = 88 ppm	Table S10 16 Structures
6	Carbamic Acid 1 amine, 0 silanols	δ_C = 153.8 ppm δ_N = 82.5 ppm	δ_C = 152.6 ppm δ_N = 88 ppm	Table S11 9 Structures
7	Ammonium Bicarbonate	δ_C = 162.0 ppm δ_N = 37.5 ppm	δ_C = 162.2 ppm δ_N = 32 ppm	Table S12 11 Structures
8	Silylpropyl-carbamate	δ_C = 147.4 ppm δ_N = 91.9 ppm	δ_C = — δ_N = 88 ppm	Table S13 4 Structures
9	Ditethered Carbamic Acid	δ_C = 158.5 ppm δ_N = 100.2 ppm	δ_C = — δ_N = —	Table S14 9 Structures

166

Carbamic acid and propylammonium carbamate

A comprehensive analysis of the CO_2 species formed upon reaction of carbon dioxide with alkylamine/alkylammonium molecules has been performed, based on DFT calculations with cluster models that include the propylcarbamic acid/propylcarbamate chain, an unreacted alkylamine/alkylammonium chain and one or more surface silanol groups (up to five silanol groups), as shown in Figure 1.

^{13}C solid-state NMR enables the distinction between carbamate ion pairs and carbamic acid, the former with a peak at 160-161 ppm and the latter at 164-165 ppm [25, 32, 34] (Table S20). The calculated ^{13}C CS of the most stable structures representing these two species have been already reported by us [32]. We have recently shown that propylammonium carbamate ion pairs could be identified by the extreme sensitivity of ^{13}C chemical shift anisotropy (CSA) to proton transfer [47]. Moreover a model of carbamate ion pairs, where proton transfer from a COOH group to a neighbour amine was forced, could also reproduce well the experimental ^{13}C CSA tensor components [47], albeit at the expense of a high energy (i.e., 30 kJ/mol less stable) carbamate ion pair model.

184

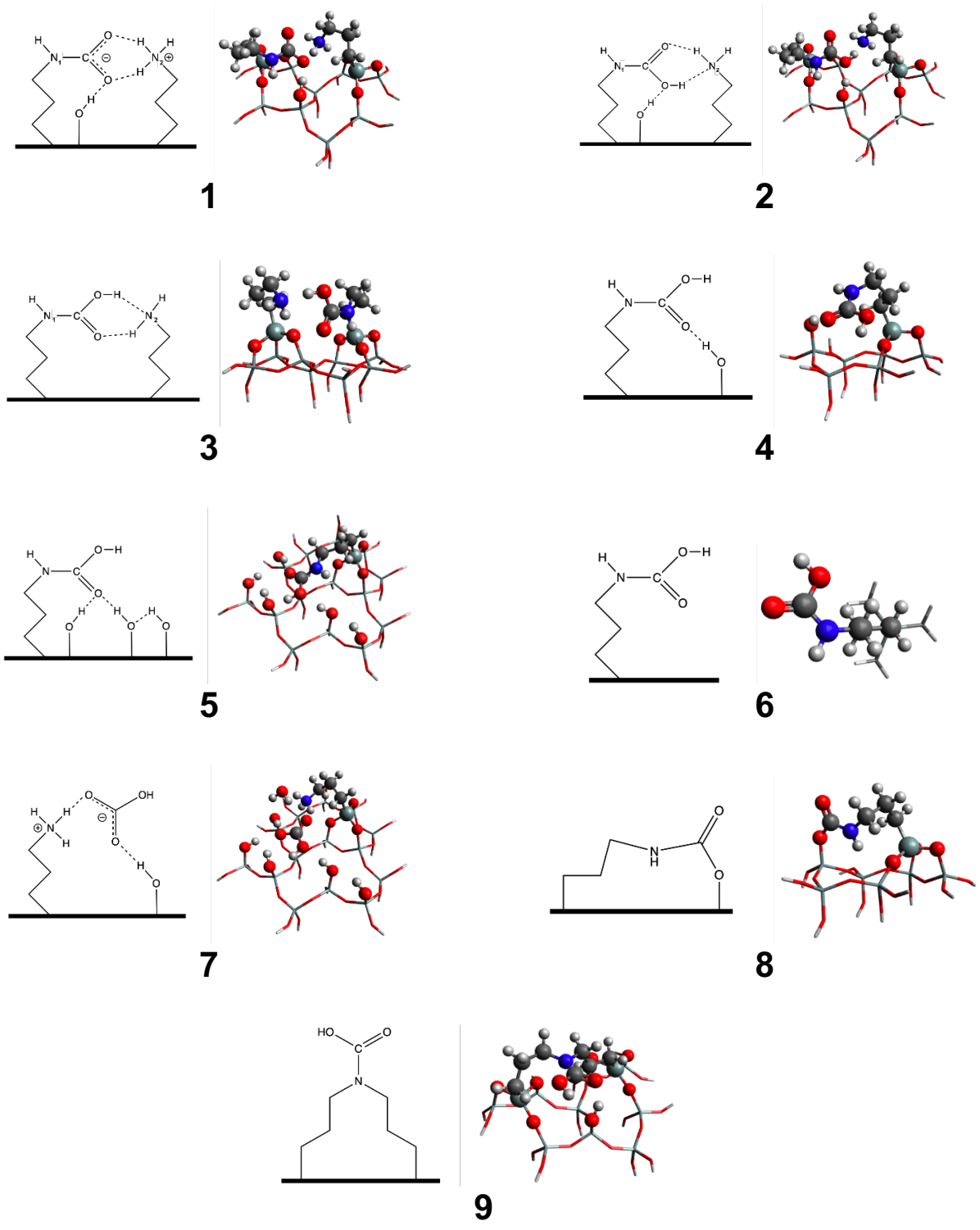

185 **Figure 1.** 2D and 3D structural representations of different CO_2-amine adducts. Corresponding
186 calculated and experimental NMR parameters are presented in Table 1. 3D representations are lowest-
187 energy optimised structures. Stick and ball-and-stick representations denote frozen and fully optimised

atoms, respectively. Colour code is: white, H; dark grey, C; blue, N; red, O; and light grey, Si. Numbering as in Table 1.

It was possible to find in this work, models of carbamic acid and carbamate structures possessing very similar stabilities (with the latter being less stable than the former by only 3.6 kJ/mol, Table S16). Several different initial configurations containing alkylammonium carbamate ion pairs were built albeit the geometry optimisation runs originated neutral species at the end. Ionic species could only be studied by freezing the three N-H bond lengths of the ammonium species to 1.017 Å. However, it is worth mentioning that one of the initial structures (**1,** Figure 1) led to the formation of the ammonium carbamate ion pair without imposing geometrical restrictions. Indeed, this was the only initial model from the dozens studied in this and in our previous works where the charged species were stable without necessitating to freeze the three N-H bond lengths of the ammonium species. This shows the important role that hydrogen networks may have on the stabilisation of the distinct carbonaceous surface species. In this case, there is a silanol species in the neighbourhood of the carbamate ion that stabilizes the ammonium carbamate ion pair. In fact, the obtained carbamate ion pair model exhibited much lower Gibbs energy than those reported in the previous works. The conformer obtained is thus another strong indication that the commonly observed ^{13}C resonance at δ ~ 164.3 ppm (δ_{calc} = 163.7 ppm), labelled as **C** in the ^{13}C CPMAS spectra of Figure 2, corresponds to an alkylammonium carbamate ion pair. The nitrogen nucleus of the carbamate moiety of the corresponding structure (**1**) resonates at δ_{calc} (^{15}N) = 90.4 ppm (δ_{exptl} ~ 88 ppm).

^{15}N CPMAS NMR spectra in two recent studies [34-35] have shown that carbamic acid and propylammonium carbamate contribute to a single resonance at 88 ppm. The

calculated ^{15}N CS of the various models considered for these two species, which are listed in Table 1, are in good agreement with this experimental result.

$^{15}N\{^{13}C\}$ rotational-echo double-resonance (REDOR) data has also been employed to show that labelled carbon dioxide binds to the amine group, resonating at 88 ppm (^{15}N), and to derive an internuclear ^{15}N-^{13}C distance of 1.45 Å [34]. A similar distance was obtained by Huang et al. [42]. However, in our structural models of carbamic acid and ammonium carbamate, N-C distances around 1.36-1.37 Å were obtained, a range that is, nevertheless, in close agreement with the typical distances observed for carbamate [56-59] and carbamic acid [60-61] crystallographic structures.

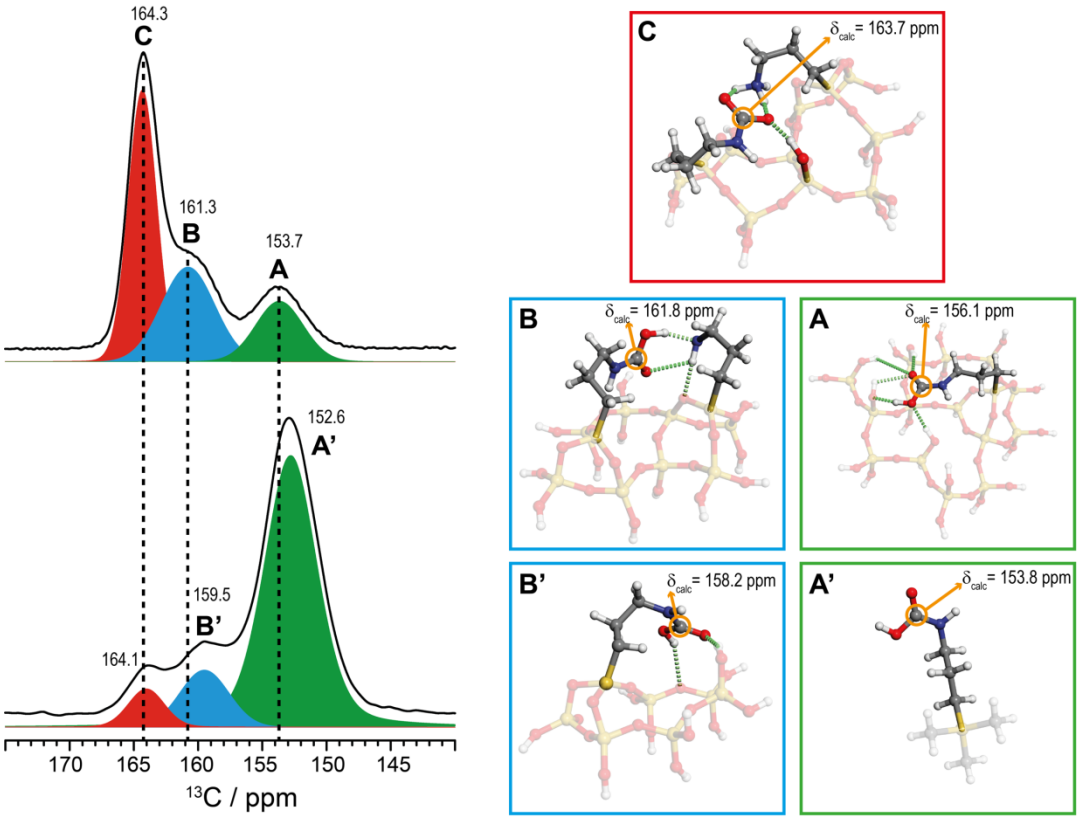

Figure 2. Left: ^{13}C CPMAS NMR spectra of $^{13}CO_2$-loaded APTES@SBA-15 (mesoporous silica) with high (**top**) and low (**bottom**) amine loadings. **Right**: Clusters used to model the different ^{13}C resonances present in the two spectra. A' and B' are used to represent the A and B resonances in the low amine

loading spectrum (**bottom**). Colour code for atoms: grey, C; red, O; blue, N; white, H; yellow, Si. The silica surface model was intentionally faded out to better emphasize the propylamine chains. Resonance C is associated with model **1** from Figure 1, resonance B with **3**, resonance B' with **4**, resonance A with **5** and resonance A' with **6**.

Many authors, including us, have tried to investigate how amine loading impacts the nature of CO_2 species formed in silica-based materials [29, 47, 62-63]; however, computational studies modelling CO_2 structures in conditions of high- and low-amine loadings are extremely scarce [42]. Whether CO_2 species are isolated or establishing hydrogen bonds with neighbouring amines, with or without the involvement of hydrogen bonded silanol groups, is still very debatable and very difficult to verify through experimental evidence. To shed light on this matter, it is highly convenient to study materials with the highest and lowest (without compromising detection limits associated to certain spectroscopic techniques) possible amounts of amine coverage in common silica-based materials. To achieve this goal, two amine-functionalized SBA-15 materials have been prepared. One where the amine loading is relatively high, *i.e.*, 2.8 mmol·g^{-1}, and a second where chemical control of amine-amine distances has been performed through the insertion of "bulky" tert-butylcarbamate protecting group into 3-aminopropyltriethoxysilane (APTES) prior to the grafting procedure, which is then readily released upon heating, leaving behind isolated amine groups grafted within the pores. The synthetic route to accomplish this chemical transformation has been taken from ref. [47] and yielded 0.5 mmol of amines per gram of SBA-15 material. This ensures that amines are at least sufficiently spaced from each other. Figure 2 shows how the ^{13}C CPMAS NMR spectra are affected by this modification.

Figure 2 depicts the full assignment of the ^{13}C resonances in a sample that was meticulously prepared by packing the NMR rotor (sample holder) under rigorous conditions that warrant complete absence of moisture and full control of CO_2 partial pressures [47]. In materials containing high-amine loadings, it was shown that species **A** and **B** are both associated to carbamic acid [32, 47]. Interestingly, while **C** species appears approximately at the same CS position, regardless of the amine loading employed (Figure 2), resonances **A** and **B** become slightly shifted to a lower CS region (**A'** and **B'**) upon amine dilution. The difference is markedly visible for resonance **B→B'**, which shifts almost 2 ppm. Note that the intensities of resonances **C** and **B** are inverted with respect to **A** when the NMR spectra associated to the high- and low-amine loadings are compared. This seems to indicate that paired amines (**B** and **C**) become scarce or vanish upon amine dilution. To check whether the observed ^{13}C resonance shifts, at low amine loadings, are associated to the loss of paired CO_2 species (*i.e.*, only isolated carbamic acid species are favoured), new cluster models have been generated to calculate ^{13}C CS in various conformations of non-paired carbamic acid. We denote these new models as **B'** and **A'** in the rightmost side of Figure 2.

Isolated carbamic acid (non-paired) was modelled using different silica surface chemical environments; i) gas phase (*i.e.*, not interacting with any silanol), ii) interacting with one Si-OH and iii) interacting with an excess of Si-OH (up to five silanol groups). The lowest-energy models are shown in Figure 1. All the other models containing different combinations of silanol groups can be found in Tables S7-S11, ranked by their total energies.

A model capable of reproducing the experimental ^{13}C CS of resonances **C** (164.3 ppm) and **B** (161.3 ppm), could not be reached among the generated non-paired carbamic

acid models (Table S9-S11), except for much higher-energy clusters from which resonance **B** could be modelled. It is remarkable that the two lowest-energy models obtained for isolated carbamic acid (Table 1 and Figure 1, **4** and **6**) fit very well the experimental CS values of resonances **A'** (δ_{exptl} = 152.6 ppm *vs.* δ_{calc} = 153.8 ppm) and **B'** (δ_{exptl} = 159.5 ppm *vs.* δ_{calc} = 158.2 ppm). It should be mentioned that model **6** refers to a gas phase carbamic acid, which is hypothesised to model a scenario where hydrogen bonding involving silanol groups is not possible. Note that this was the only model that best-fit the experimental resonance **A'** further supporting the fact that this isolated CO_2 species is not interacting with oxygen atoms in its vicinity.

Although resonances **A'** and **B'**, appearing in the ^{13}C CPMAS NMR spectrum of the sample treated to quench the pairing of propylamines, are very likely associated with isolated CO_2 species, we shall remain sceptical and cannot disregard the possibility to form minor quantities of paired amines that could give rise to CO_2 species resonating at similar frequencies. However, given that resonance **C** does not shift makes sense because: i) this is the CO_2 species associated to ammonium carbamate ion pairs, where amine pairing is mandatory for its existence, and ii) this resonance becomes the species with the smallest intensity, which is fully compatible with the idea of having only a very small quantity of paired amines "surviving" under conditions of extreme amine dilution.

Overall, the DFT models of "paired" and "isolated" CO_2 species seem to explain the slightly shielded resonances **A** and **B** (to become **A'** and **B'**), while **C** remains in the same CS upon amine dilution. This leads us to conclude that CO_2 speciation can be far more complex than expected. In fact, several distinct CO_2 species can co-exist depending on the number of silanol groups neighbouring the grafted amines, and on the possibility of eventual amine-amine pairing.

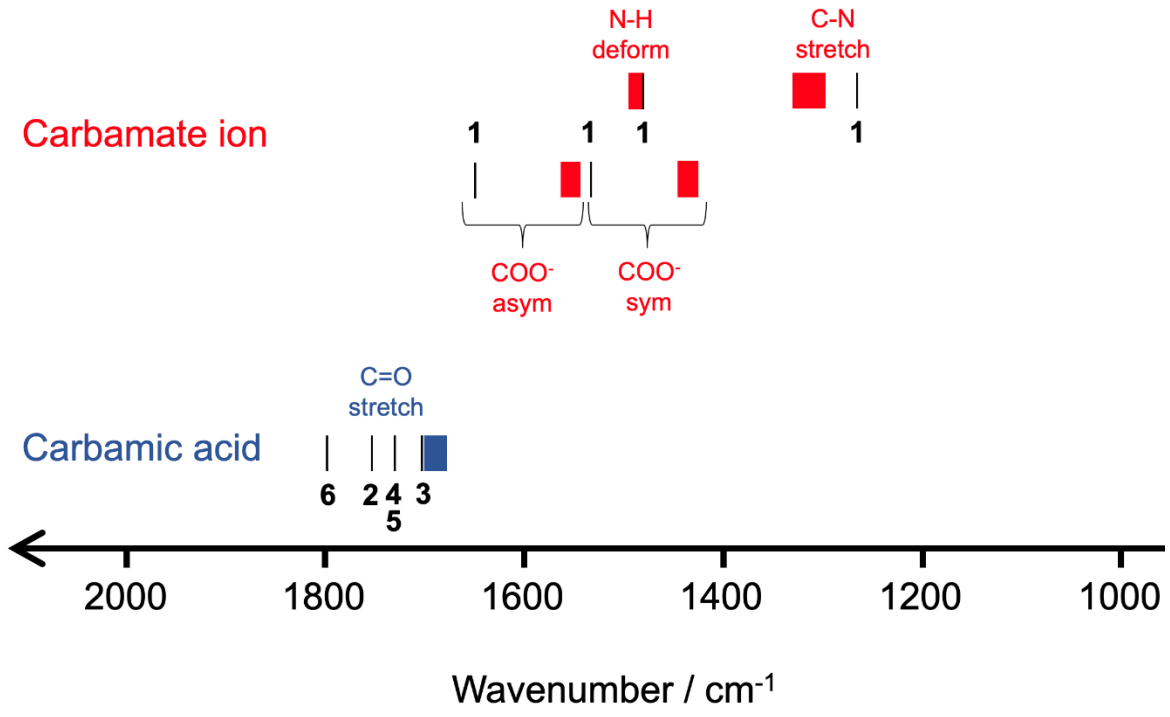

Figure 3. Typical ranges (filled boxes) of characteristic wavenumbers of carbamic acid and carbamate ion, collected from experiments in the literature [19, 21, 23-24, 29, 31, 33, 54, 63-66]. Corresponding calculated values from this work (labelling as in Figure 1 and wavenumbers in Table S21) are represented by black lines.

A significant number of studies involving CO_2 speciation in amine-functionalised silicas has been performed using FTIR spectroscopy. The DFT models used to compute the NMR CSs can also be employed in the calculation of vibrational modes to simulate FTIR spectra that can be compared with the experimental ones. We have made a comprehensive screening of infrared spectroscopic data from different literature sources [19, 21, 23-24, 29, 31, 33, 54, 63-66] and compiled the data in the diagram shown in Figure 3. This figure shows wavenumber ranges for some of the characteristic frequencies collected from literature for carbamic acid and carbamate ion, together with calculated values from the models shown in Figure 1. Overall, there is a good agreement between

calculated and experimental values of N-H deformation and C-N stretching in carbamates, with the calculated value of the latter being slightly lower compared to the experimental value. For COO^- asymmetric and symmetric stretching in the carbamate ion and C=O stretching vibrations in carbamic acid, there is a significant overestimation of the wavenumbers relative to the wavenumbers up to ~100 cm^{-1} (Table S21). The distinct carbamic acid models generate significantly different estimates for C=O stretching vibration, in a range of 94 cm^{-1}. The carbamic acid (**2**) model analogous to that of ammonium carbamate (**1**) generates an overestimation of 55 cm^{-1}.

Based on the above discussion, it is suggested that both the ion pair ammonium carbamate and the neutral pair amine-carbamic acid are typically present in aminated silicas that have come into contact with CO_2. Partial charge stabilization in ammonium carbamate necessitates a network of hydrogen-bonds involving this species, which is supported by the observation that its ^{13}C NMR resonance is remarkably constant at 164-165 ppm. The intricate network of hydrogen bonds is also compatible with its resistance to regeneration by vacuum [35]. Carbamic acid is suggested to occur on a range of varying chemical environments. While its characteristic C=O infrared frequency is tightly range-bound, the ^{13}C resonance can vary significantly with amine or silanol concentration and moisture.

Ammonium Bicarbonate

Formation of ammonium bicarbonate on the surface of amine-functionalised silicas, upon reaction with CO_2 and H_2O, has been asserted since the onset of the field [1-2]. Working with grafted primary amines, Leal et al. [2] were the first, in 1995, to provide

some sort of evidence for this claim, by identifying an infrared band at 1384 cm^{-1} associated to C-O bending in bicarbonate. In 2003, Huang et al. [67] made a similar identification with a band at 1382 cm^{-1}. Many other groups claimed to have detected bicarbonate-specific infrared bands [17-18, 20-22, 29, 33, 37-38, 46, 54, 65, 68-69], albeit band assignments reported in these studies are inconsistent. This led some authors to doubt whether bicarbonate was even formed in solid amine-functionalised materials [23-24, 70-71]. Our own results regarding the computed infrared spectrum of bicarbonate (Figure S7 and Table S24) provide some support to the previous identifications of ammonium bicarbonate in samples containing primary amines. In particular, the asymmetric and symmetric COO^- stretching vibrations, identified usually at 1670-1616 cm^{-1} and 1360-1350 cm^{-1}, respectively, seem to correlate well with calculated frequencies of 1696 cm^{-1} and 1385 cm^{-1}.

Recent studies show that the use of tertiary amines provides powerful evidence for the formation of bicarbonate in amine-functionalised silicas. For instance, Lee et al. [46] reported a ^{13}C CS of 162.2 ppm for the carbonyl resonance in bicarbonate; as the usual chemisorbed CO_2 species (carbamic acid and carbamate) are only formed in primary/secondary amines and not in bulkier amines. The same authors have also employed $^{13}C\{^{15}N\}$ REDOR NMR experiments [34], in materials grafted with primary amines, suggesting that 10 % of the observed ^{13}C resonance intensity at 165 ppm could also be associated to ammonium bicarbonate. Still, it is complicated to verify the presence or absence of ammonium bicarbonate in samples of mesoporous silicas not fully degassed (i.e., containing water) modified with primary/secondary amines due to strong resonance overlap with other CO_2 species in this ^{13}C CS region.

Our DFT results lend some support to the experimental ^{15}N CS reported elsewhere [34]. The ^{15}N CS of the most stable structure model of ammonium bicarbonate (**7**, Table 1) is somewhat larger than that of ammonium siloxide (**11**, Table S1), but not enough to decisively discern it by ^{15}N NMR. Similarly, the calculated ^{13}C CS is relatively close to the experimental value [46], *i.e.*, 162.0 and 162.2 ppm, respectively.

Our energetic analysis of the bicarbonate stability (Table S18) shows that this species is 12 kJ/mol less stable than carbamic acid, when using single-amine/single-silanol clusters. This suggests that formation of carbamic acid under wet conditions is still favoured. However, this result needs to be taken carefully, as discussed for the amine/ammonium system (see section "Alkylamine and alkylammonium chains"). In fact, it is perfectly possible that bicarbonate forms in some samples and not in others, depending on the kind and concentrations of amines and the type of host material [29, 62-63]. This could explain why some authors reported a significant increase in the CO_2 adsorption capacity of amine-functionalised materials upon introduction of water into the system [2-3, 67-69, 72-74], while others did not [19, 24, 70, 75-77].

Silylpropylcarbamate

Formation of silypropylcarbamate, also known as surface-bonded carbamate, has been proposed in previous publications [23-24, 29, 37, 63], based on interpretations of infrared spectra. Identification of this species was made based on infrared bands at 1510 cm^{-1} and 1714 cm^{-1}. These bands could easily be used to propose the formation of carbamic acid, as the authors themselves recognise. In addition, they argue carbamic acid is thermodynamically unstable, and therefore cannot be present, leaving silylpropylcarbamate as the only other alternative albeit carbamic acid has

388 been securely identified in CO_2-exposed amine-functionalised silica, using both
389 infrared [17-18, 21, 24, 29, 31, 33, 36-37, 54, 64-66] and NMR spectroscopy [25, 32, 34]. Bacsik et al. [24]
390 have made a more compelling case for the formation of silylpropylcarbamate. They
391 admitted that samples with low amine concentration might lead to the formation of
392 carbamic acid, but also added that, with time, the latter species condenses with
393 surface silanols to form silylpropylcarbamate. The authors grounded this conclusion
394 on a shift of the vibration associated with the carbonyl peak from 1704 cm^{-1} to 1715
395 cm^{-1}, from 2 to 60 min after the introduction of CO_2 into the system. Furthermore, the
396 authors observed that the species at 1715 cm^{-1} was more common in samples with
397 low amine loading and persisted upon CO_2 evacuation and high temperatures. From
398 the same group, Aziz et al. [63] used an infrared band at 1700-1695 cm^{-1} to identify the
399 presence of carbamic acid and silylpropylcarbamate, being unable to distinguish
400 between the two. Didas et al. [29] have also postulated the presence of
401 silylpropylcarbamate, although all the infrared bands used for its identification could
402 also easily be attributed to carbamic acid. Yu and Chuang [37] mentioned the possibility
403 of formation of silylpropylcarbamate, without providing any evidence. We have
404 simulated the infrared spectrum considering a silylpropylcarbamate model (**8,** Figure
405 1); the calculated frequencies at 1799 and 1479 cm^{-1} (Figure S6 and Table S23),
406 correspond to C=O stretching and N-H bending modes, respectively. These theoretical
407 vibrational bands do not correlate well with experimental values obtained by the
408 different authors. Our calculations show that the calculated C=O stretching vibration
409 for silylpropylcarbamate is overestimated up to ~ 100 cm^{-1} (1700 vs 1799 cm^{-1}),
410 considering that the experimental band at *ca.* 1700 is correctly assigned to this
411 species. This discrepancy further emphasizes how difficult it is to reach definite

assignment of CO_2 species on such a complex matrix based solely on FTIR measurements.

Very similar calculated ^{15}N CS ranging from 91.9 to 98.5 ppm (Table S13), were obtained for models of silylpropylcarbamate; the lower ^{15}N CS limit is rather close to the experimental value (88 ppm) reported by Shimon et al. [35].The same comparison cannot be made through ^{13}C CS analysis as there is no ^{13}C resonance that can be assigned to this species. In fact, according to our lowest energy model (**8**, Figure 1), the calculated ^{13}C CS of the silylpropylcarbamate carbonyl yields 147.4 ppm (Table 1), which is well outside the typical range of ^{13}C CS associated to the observed CO_2 species (Figure 2 and Table S20). In addition, the energetic analysis of silylpropylcarbamate (Table S17) shows it to be 30 kJ/mol less stable than carbamic acid, and 15 kJ/mol less stable than adsorbed CO_2, which are significant differences, suggesting that the formation of silylpropylcarbamate in amine-functionalised silicas is thermodynamically unfavourable. Therefore, our results do not support the presence of this species as it was hypothesised by other authors.

Ditethered carbamic acid

Previous works [34-35] assigned the ^{15}N resonance at 44 ppm to unreactive ditethered amine (secondary amine) species showing that this species remains unchanged upon adsorption/desorption of CO_2. It was suggested in those works that this could be due to the rigidity of the ditethered chain, since secondary amines typically readily react with CO_2. Our results show that ditethered carbamic acid lowest-energy model (**9**, Figure 1) give rise to a ^{15}N CS at 100.2 ppm, which is *ca.* 10 ppm higher than those obtained for single-tethered carbamic acid (δ_N=91.2 ppm) and alkylammonium

carbamate (δ_N = 90.4 ppm) models (Table 1). This is fully consistent with previous interpretations where the experimental ^{15}N CS of CO_2-adducts resonates at δ_N ~ 88 ppm [34-35], which is quite far from the calculated value (100.2 ppm). The energy penalty obtained upon the formation of ditethered carbamic acid (**9**), compared to a free amine with nearby physisorbed CO_2 (**12**, Figure S2), is 70 kJ/mol (Table S19). Thus, the formation of ditethered carbamic acid upon adsorption of CO_2 into a silica adsorbent with doubly-grafted amines is excluded.

Since hydrogen bonds are fundamental to stabilise the structure of single-tethered carbamic acid, ditethered amine motion is probably hindered to such an extent (when compared to single-tethered amines) that interactions with the surface become difficult, and can only occur with significant straining of the alkyl chains. The hydrogen bond stabilising effect thus seems to be missing in ditethered carbamic acid, explaining the lower stability of this species. A previous study also suggested that interactions with the surface are central to the stabilisation of amine-CO_2 adducts [23].

In summary, in this work, an exhaustive survey of the most relevant atomic level studies regarding the chemisorbed CO_2 structure is provided. We revisit the experimental proofs of assignment of the distinct chemisorbed CO_2 species found thus far in the literature by debating results obtained from different authors, highlighting, whenever possible, controversial assignments regarding the existence of certain chemisorbed CO_2 species. A number of structural aspects regarding the formation of certain CO_2 species in mesoporous aminosilicas functionalized with distinct amine loadings have also been revisited by means of DFT calculations of NMR and FTIR parameters based on chemisorbed CO_2 structure models. In particular, the M06-2X functional was used to calculate ^{15}N and ^{13}C NMR CSs, FTIR spectra and Gibbs energies of formation for several CO_2 species that may be present in pristine and CO_2-

loaded aminosilicas. Several structural models were analysed for the first time while others were revisited in order to compare experimental and calculated $^{13}C/^{15}N$ CSs and vibrational modes. Calculated Gibbs energies of formation were typically good indicators of the propensity of such species to form, i.e, carbamic acid and carbamate moieties are slightly more stable than bicarbonate, and significantly more stable than silylpropylcarbamate or ditethered carbamic acid, in decreasing ordering of stability. ^{15}N CSs confirmed the presence of three possible species of amine/ammonium in the samples prior to the introduction of CO_2 into the system, *i.e.*, amine, ammonium siloxide and ditethered amine. Calculated ^{13}C CSs, coupled with an experimental assessment, confirmed the formation of several kinds of carbamic acid/carbamate moieties, in CO_2-loaded materials containing distinct amine loadings. Simulated infrared spectra of carbamic acid and alkylamonium carbamate compared well with typical experimental values, confirming these to be the predominant CO_2 species.

Acknowledgements

This work was developed in the scope of the projects CICECO-Aveiro Institute of Materials POCI-01-0145-FEDER-007679 (Ref. FCT UID/CTM/50011/2019), PRESSNMR_MAT - P2020-PTDC/QEQ-QAN/6373/2014, GAS2MAT-DNPSENS - POCI-01-0145-FEDER-028747 and Smart Green Homes POCI-01-0247-FEDER-007678, a co-promotion between Bosch Termotecnologia S.A. and the University of Aveiro. These projects are financed by Portugal 2020 under the Competitiveness and Internationalization Operational Program and by the European Regional Development

Fund (FEDER). The authors are also thankful to Fundação para a Ciência e a Tecnologia (FCT) for the Investigator FCT program (LM and JRBG).

Supporting Information

Experimental details, optimised structures and chemical shifts of alkylammonium and alkylamine chains, detailed optimisation results, energetic analysis of the relative stability of different species, simulated infrared spectra of different species, root-mean-square error of ^{15}N chemical shift calculation and three-dimensional structure of the glycine cluster used to model the crystal structure of α-glycine. The Supporting Information is available free of charge on the ACS Publications website at DOI: 10.1021/ …

References

1. Leal, O.; Bolivar, C.; Sepúlveda, G.; Molleja, G.; Martínez, G.; Esparragoza, L. Carbon Dioxide Adsorbent and Method for Producing the Adsorbent. U.S. Patent 5087597, 1992.
2. Leal, O.; Bolivar, C.; Ovalles, C.; Garcia, J. J.; Espidel, Y., Reversible adsorption of carbon dioxide on amine surface-bonded silica gel. *Inorg. Chim. Acta* **1995,** *240*, 183-189.
3. Satyapal, S.; Filburn, T.; Trela, J.; Strange, J., Performance and Properties of a Solid Amine Sorbent for Carbon Dioxide Removal in Space Life Support Applications. *Energy Fuels* **2001,** *15*, 250-255.
4. Xu, X.; Song, C.; Andresen, J. M.; Miller, B. G.; Scaroni, A. W., Novel Polyethylenimine-Modified Mesoporous Molecular Sieve of MCM-41 Type as High-Capacity Adsorbent for CO2 Capture. *Energy Fuels* **2002,** *16*, 1463-1469.
5. Younas, M.; Sohail, M.; Kong, L. L.; Bashir, M. J. K.; Sethupathi, S., Feasibility of CO2 adsorption by solid adsorbents: a review on low-temperature systems. *Int. J. Environ. Sci. Technol.* **2016,** *13*, 1839-1860.
6. Wang, J.; Huang, L.; Yang, R.; Zhang, Z.; Wu, J.; Gao, Y.; Wang, Q.; O'Hare, D.; Zhong, Z., Recent advances in solid sorbents for CO2 capture and new development trends. *Energy Environ. Sci.* **2014,** *7*, 3478-3518.
7. Chen, C.; Zhang, S.; Row, K. H.; Ahn, W.-S., Amine–silica composites for CO2 capture: A short review. *J. Energy Chem.* **2017,** *26*, 868-880.
8. Sanz-Pérez, E. S.; Murdock, C. R.; Didas, S. A.; Jones, C. W., Direct Capture of CO2 from Ambient Air. *Chem. Rev.* **2016,** *116*, 11840-11876.
9. Gebald, C.; Repond, N.; Wurzbacher, J. A. Steam Assisted Vacuum Desorption Process for Carbon Dioxide Capture. U.S. Patent 0203249 A1, 2017.
10. Gebald, C.; Meier, W.; Repond, N.; Ruesch, T.; Wurzbacher, J. A. Direct Air Capture Device. U.S. Patent 0106330 A1, 2017.
11. Choi, S.; Drese, J. H.; Chance, R. R.; Eisenberger, P. M.; Jones, C. W. Application of Amine-Tethered Sold Sorbents to CO2 Fixation from Air. U.S. Patent 8491705 B2, 2013.
12. Eisenberger, P. System and Method for Carbon Dioxide Capture and Sequestration. U.S. Patent 8500855 B2, 2013.
13. Bhattacharyya, D.; Miller, D. C., Post-combustion CO2 capture technologies — a review of processes for solvent-based and sorbent-based CO2 capture. *Curr. Opin. Chem. Eng.* **2017,** *17*, 78-92.
14. Modak, A.; Jana, S., Advancement in porous adsorbents for post-combustion CO2 capture. *Micropor. Mesopor. Mater.* **2019,** *276*, 107-132.
15. Zhao, X.; Cui, Q.; Wang, B.; Yan, X.; Singh, S.; Zhang, F.; Gao, X.; Li, Y., Recent progress of amine modified sorbents for capturing CO2 from flue gas. *Chin. J. Chem. Eng.* **2018,** *26*, 2292-2302.
16. Zhang, G.; Zhao, P.; Xu, Y.; Yang, Z.; Cheng, H.; Zhang, Y., Structure Property-CO2 Capture Performance Relations of Amine-Functionalized Porous Silica Composite Adsorbents. *ACS Appl. Mater. Interfaces* **2018,** *10*, 34340-34354.
17. Chang, A. C. C.; Chuang, S. S. C.; Gray, M.; Soong, Y., In-Situ Infrared Study of CO2 Adsorption on SBA-15 Grafted with γ-(Aminopropyl)triethoxysilane. *Energy Fuels* **2003,** *17*, 468-473.

18. Khatri, R. A.; Chuang, S. S. C.; Soong, Y.; Gray, M., Carbon Dioxide Capture by Diamine-Grafted SBA-15: A Combined Fourier Transform Infrared and Mass Spectrometry Study. *Ind. Eng. Chem. Res.* **2005,** *44*, 3702-3708.
19. Hiyoshi, N.; Yogo, K.; Yashima, T., Adsorption characteristics of carbon dioxide on organically functionalized SBA-15. *Micropor. Mesopor. Mater.* **2005,** *84*, 357-365.
20. Khatri, R. A.; Chuang, S. S. C.; Soong, Y.; Gray, M., Thermal and Chemical Stability of Regenerable Solid Amine Sorbent for CO2 Capture. *Energy Fuels* **2006,** *20*, 1514-1520.
21. Knöfel, C.; Martin, C.; Hornebecq, V.; Llewellyn, P. L., Study of Carbon Dioxide Adsorption on Mesoporous Aminopropylsilane-Functionalized Silica and Titania Combining Microcalorimetry and in Situ Infrared Spectroscopy. *J. Phys. Chem. C* **2009,** *113*, 21726-21734.
22. Sayari, A.; Belmabkhout, Y., Stabilization of Amine-Containing CO2 Adsorbents: Dramatic Effect of Water Vapor. *J. Am. Chem. Soc.* **2010,** *132*, 6312-6314.
23. Danon, A.; Stair, P. C.; Weitz, E., FTIR Study of CO2 Adsorption on Amine-Grafted SBA-15: Elucidation of Adsorbed Species. *J. Phys. Chem. C* **2011,** *115*, 11540-11549.
24. Bacsik, Z.; Ahlsten, N.; Ziadi, A.; Zhao, G.; Garcia-Bennett, A. E.; Martín-Matute, B. e.; Hedin, N., Mechanisms and Kinetics for Sorption of CO2 on Bicontinuous Mesoporous Silica Modified with n-Propylamine. *Langmuir* **2011,** *27*, 11118-11128.
25. Pinto, M. L.; Mafra, L. s.; Guil, J. M.; Pires, J.; Rocha, J., Adsorption and Activation of CO2 by Amine-Modified Nanoporous Materials Studied by Solid-State NMR and 13CO2 Adsorption. *Chem. Mater.* **2011,** *23*, 1387-1395.
26. Bollini, P.; Didas, S. A.; Jones, C. W., Amine-oxide hybrid materials for acid gas separations. *J. Mater. Chem.* **2011,** *21*, 15100-15120.
27. Sayari, A.; Belmabkhout, Y.; Da'na, E., CO2 Deactivation of Supported Amines: Does the Nature of Amine Matter? *Langmuir* **2012,** *28*, 4241-4247.
28. Sayari, A.; Heydari-Gorji, A.; Yang, Y., CO2-Induced Degradation of Amine-Containing Adsorbents: Reaction Products and Pathways. *J. Am. Chem. Soc.* **2012,** *134*, 13834-13842.
29. Didas, S. A.; Sakwa-Novak, M. A.; Foo, G. S.; Sievers, C.; Jones, C. W., Effect of Amine Surface Coverage on the Co-Adsorption of CO2 and Water: Spectral Deconvolution of Adsorbed Species. *J. Phys. Chem. Lett.* **2014,** *5*, 4194-4200.
30. Moore, J. K.; Sakwa-Novak, M. A.; Chaikittisilp, W.; Mehta, A. K.; Conradi, M. S.; Jones, C. W.; Hayes, S. E., Characterization of a Mixture of CO2 Adsorption Products in Hyperbranched Aminosilica Adsorbents by 13C Solid-State NMR. *Environ. Sci. Technol.* **2015,** *49*, 13684-13691.
31. Hahn, M. W.; Jelic, J.; Berger, E.; Reuter, K.; Jentys, A.; Lercher, J. A., Role of Amine Functionality for CO2 Chemisorption on Silica. *J. Phys. Chem. B* **2016,** *120*, 1988-1995.
32. Mafra, L.; Čendak, T.; Schneider, S.; Wiper, P. V.; Pires, J.; Gomes, J. R. B.; Pinto, M. L., Structure of Chemisorbed CO2 Species in Amine-Functionalized Mesoporous Silicas Studied by Solid-State NMR and Computer Modeling. *J. Am. Chem. Soc.* **2017,** *139*, 389-408.
33. Foo, G. S.; Lee, J. J.; Chen, C.-H.; Hayes, S. E.; Sievers, C.; Jones, C. W., Elucidation of Surface Species through in Situ FTIR Spectroscopy of Carbon Dioxide Adsorption on Amine-Grafted SBA-15. *Chem. Sus. Chem.* **2017,** *10*, 266-276.
34. Chen, C.-H.; Shimon, D.; Lee, J. J.; Didas, S. A.; Mehta, A. K.; Sievers, C.; Jones, C. W.; Hayes, S. E., Spectroscopic Characterization of Adsorbed 13CO2 on 3-Aminopropylsilyl-Modified SBA15 Mesoporous Silica. *Environ. Sci. Technol.* **2017,** *51*, 6553-6559.
35. Shimon, D.; Chen, C.-H.; Lee, J. J.; Didas, S. A.; Sievers, C.; Jones, C. W.; Hayes, S. E., 15N Solid State NMR Spectroscopic Study of Surface Amine Groups for Carbon Capture: 3-

588 Aminopropylsilyl Grafted to SBA-15 Mesoporous Silica. *Environ. Sci. Technol.* **2018,** *52*, 1488-
589 1495.
590 36. Wang, X.; Schwartz, V.; Clark, J. C.; Ma, X.; Overbury, S. H.; Xu, X.; Song, C., Infrared
591 Study of CO2 Sorption over "Molecular Basket" Sorbent Consisting of Polyethylenimine-
592 Modified Mesoporous Molecular Sieve. *J. Phys. Chem. C* **2009,** *113*, 7260-7268.
593 37. Yu, J.; Chuang, S. S. C., The Structure of Adsorbed Species on Immobilized Amines in
594 CO2 Capture: An in Situ IR Study. *Energy Fuels* **2016,** *30*, 7579-7587.
595 38. Zhang, H.; Goeppert, A.; Olah, G. A.; Prakash, G. K. S., Remarkable effect of moisture
596 on the CO2 adsorption of nano-silica supported linear and branched polyethylenimine. *J. CO2*
597 *Utilization* **2017,** *19*, 91-99.
598 39. Bernin, D.; Hedin, N., Perspectives on NMR studies of CO2 adsorption. *Curr. Opin.*
599 *Colloid Interface Sci.* **2018,** *33*, 53-62.
600 40. Young, P. D.; Notestein, J. M., The Role of Amine Surface Density in Carbon Dioxide
601 Adsorption on Functionalized Mixed Oxide Surfaces. *Chem. Sus. Chem.* **2011,** *4*, 1671-1678.
602 41. Mello, M. l. R.; Phanon, D.; Silveira, G. Q.; Llewellyn, P. L.; Ronconi, C. l. M., Amine-
603 modified MCM-41 mesoporous silica for carbon dioxide capture. *Micropor. Mesopor. Mater.*
604 **2011,** *143*, 174-179.
605 42. Huang, S.-J.; Hung, C.-T.; Zheng, A.; Lin, J.-S.; Yang, C.-F.; Chang, Y.-C.; Deng, F.; Liu, S.-
606 B., Capturing the Local Adsorption Structures of Carbon Dioxide in Polyamine-Impregnated
607 Mesoporous Silica Adsorbents. *J. Phys. Chem. Lett.* **2014,** *5*, 3183-3187.
608 43. Santos, T. C. d.; Bourrelly, S.; Llewellyn, P. L.; Carneiro, J. W. d. M.; Ronconi, C. M.,
609 Adsorption of CO2 on amine-functionalised MCM-41: experimental and theoretical studies.
610 *Phys. Chem. Chem. Phys.* **2015,** *17*, 11095-11102.
611 44. Hung, C.-T.; Yang, C.-F.; Lin, J.-S.; Huang, S.-J.; Chang, Y.-C.; Liu, S.-B., Capture of carbon
612 dioxide by polyamine-immobilized mesostructured silica: A solid-state NMR study. *Micropor.*
613 *Mesopor. Mater.* **2017,** *238*, 2-13.
614 45. Milner, P. J.; Siegelman, R. L.; Forse, A. C.; Gonzalez, M. I.; Runcěvski, T.; Martell, J. D.;
615 Reimer, J. A.; Long, J. R., A Diaminopropane-Appended Metal−Organic Framework Enabling
616 Efficient CO2 Capture from Coal Flue Gas via a Mixed Adsorption Mechanism. *J. Am. Chem.*
617 *Soc.* **2017,** *139*, 13541-13553.
618 46. Lee, J. J.; Chen, C.-H.; Shimon, D.; Hayes, S. E.; Sievers, C.; Jones, C. W., Effect of
619 Humidity on the CO2 Adsorption of Tertiary Amine Grafted SBA-15. *J. Phys. Chem. C* **2017,**
620 *121*, 23480-23487.
621 47. Čendak, T.; Sequeira, L.; Sardo, M.; Valente, A.; Pinto, M. s. L.; Mafra, L. s., Detecting
622 proton-transfer in CO2 species chemisorbed on amine- modified mesoporous silicas using 13C
623 NMR chemical shift anisotropy and smart control of amine surface density. *Chem. Eur. J.* **2018,**
624 *24*, 10136-10145.
625 48. Moschetta, E. G.; Sakwa-Novak, M. A.; Greenfield, J. L.; Jones, C. W., Post-Grafting
626 Amination of Alkyl Halide-Functionalized Silica for Applications in Catalysis, Adsorption, and
627 15N NMR Spectroscopy. *Langmuir* **2015,** *31*, 2218-2227.
628 49. Mafra, L.; Čendak, T.; Schneider, S.; Wiper, P. V.; Pires, J. o.; Gomes, J. R. B.; Pinto, M.
629 s. L., Amine functionalized porous silica for CO2/CH4 separation by adsorption: Which amine
630 and why. *Chem. Eng. J.* **2018,** *336*, 612-621.
631 50. Choi, M.; Kleitz, F.; Liu, D.; Lee, H. Y.; Ahn, W.-S.; Ryoo, R., Controlled Polymerization
632 in Mesoporous Silica toward the Design of Organic-Inorganic Composite Nanoporous
633 Materials. *J. Am. Chem. Soc.* **2005,** *127*, 1924-1932.

51. Samultsev, D. O.; Semenov, V. A.; Krivdin, L. B., On the accuracy of the GIAO-DFT calculation of 15N NMR chemical shifts of the nitrogen- containing heterocycles – a gateway to better agreement with experiment at lower computational cost. *Magn. Reson. Chem.* **2014,** *52*, 222-230.
52. Chapyshev, S. V.; Ushakov, E. N.; Chernyak, A. V., 15N NMR spectra and reactivity of 2,4,6- triazidopyridines, 2,4,6-triazidopyrimidine and 2,4,6-triazido-s-triazine. *Magn. Reson. Chem.* **2013,** *51*, 562-568.
53. Chapyshev, S. V.; Chernyak, A. V.; Ushakov, E. N., 13C and 15N NMR spectra of high-energy polyazidocyanopyridines. *Magn. Reson. Chem.* **2016,** *55*, 99-105.
54. Mouline, Z.; Asai, K.; Daiko, Y.; Honda, S.; Bernard, S.; Iwamoto, Y., Amine-functionalized polycarbosilane hybrids for CO2-selective membranes. *J. Eur. Ceram. Soc.* **2017,** *37*, 5213-5221.
55. Stefanovich, E. V.; Boldyrev, A. I.; Truong, T. N.; Simons, J., Ab Initio Study of the Stabilization of Multiply Charged Anions in Water. *J. Phys. Chem. B* **1998,** *201*, 4205-4208.
56. Adams, J. M.; Small, R. W. H., The crystal structure of ammonium carbamate. *Acta Crystallogr., Sect. B: Struct. Sci. Cryst. Eng. Mater.* **1973,** *29*, 2317-2319.
57. Bracher, B. H.; Small, R. W. H., The crystal structure of ethyl carbamate. *Acta Cryst.* **1967,** *23*, 410-418.
58. Cañellas, S.; Ayats, C.; Henseler, A. H.; Pericàs, M. A., CCDC 1577682: Experimental Crystal Structure Determination. **2017**.
59. Ma, Z.; Day, C. S.; Bierbach, U., CCDC 657432: Experimental Crystal Structure Determination. 2014.
60. Pesenti, C.; Bravo, P.; Corradi, E.; Frigerio, M.; Meille, S. V.; Panzeri, W.; Viani, F.; Zanda, M., CCDC 176640: Experimental Crystal Structure Determination. **2014**.
61. Siwicka, A.; Moleda, Z.; Wojtasiewicz, K.; Zawadzka, A.; Maurin, J. K.; Panasiewicz, M.; Pacuszka, T.; Czarnocki, Z., CCDC 667929: Experimental Crystal Structure Determination. 2014.
62. Aziz, B.; Zhao, G.; Hedin, N., Carbon Dioxide Sorbents with Propylamine Groups-Silica Functionalized with a Fractional Factorial Design Approach. *Langmuir* **2011,** *27*, 3822-3834.
63. Aziz, B.; Hedin, N.; Bacsik, Z., Quantification of chemisorption and physisorption of carbon dioxide on porous silica modified by propylamines: Effect of amine density. *Micropor. Mesopor. Mater.* **2012,** *159*, 42-49.
64. Tumuluri, U.; Isenberg, M.; Tan, C.-S.; Chuang, S. S. C., In Situ Infrared Study of the Effect of Amine Density on the Nature of Adsorbed CO2 on Amine-Functionalized Solid Sorbents. *Langmuir* **2014,** *30*, 7405-7413.
65. Potter, M. E.; Cho, K. M.; Lee, J. J.; Jones, C. W., Role of Alumina Basicity in CO2 Uptake in 3-Aminopropylsilyl-grafted Alumina Adsorbents. *Chem. Sus. Chem.* **2017,** *10*, 2192-2201.
66. Bacsik, Z.; Atluri, R.; Garcia-Bennett, A. E.; Hedin, N., Temperature-Induced Uptake of CO2 and Formation of Carbamates in Mesocaged Silica Modified with n-Propylamines. *Langmuir* **2010,** *26*, 10013-10024.
67. Huang, H. Y.; Yang, R. T.; Chinn, D.; Munson, C. L., Amine-Grafted MCM-48 and Silica Xerogel as Superior Sorbents for Acidic Gas Removal from Natural Gas. *Ind. Eng. Chem. Res.* **2003,** *42*, 2427-2433.
68. Serna-Guerrero, R.; Da'na, E.; Sayari, A., New Insights into the Interactions of CO2 with Amine-Functionalized Silica. *Ind. Eng. Chem. Res.* **2008,** *47*, 9406–9412.

69. Zelenak, V.; Halamova, D.; Gaberova, L.; Bloch, E.; Llewellyn, P., Amine-modified SBA-12 mesoporous silica for carbon dioxide capture: Effect of amine basicity on sorption properties. *Micropor. Mesopor. Mater.* **2008,** *116*, 358-364.
70. Hiyoshi, N.; Yogo, K.; Yashima, T., Reversible Adsorption of Carbon Dioxide on Amine-Modified SBA-15 from Flue Gas Containing Water Vapor. *Stud. Surf. Sci. Catal.* **2004,** *153*, 417-422.
71. Bacsik, Z.; Hedin, N., Effects of carbon dioxide captured from ambient air on the infrared spectra of supported amines. *Vib. Spectrosc.* **2016,** *87*, 215-221.
72. Xu, X.; Song, C.; Miller, B. G.; Scaroni, A. W., Influence of Moisture on CO2 Separation from Gas Mixture by a Nanoporous Adsorbent Based on Polyethylenimine-Modified Molecular Sieve MCM-41. *Ind. Eng. Chem. Res.* **2005,** *44*, 8113-8119.
73. Belmabkhout, Y.; Serna-Guerrero, R.; Sayari, A., Amine-bearing mesoporous silica for CO2 removal from dry and humid air. *Chem. Eng. Sci.* **2010,** *65*, 3695-3698.
74. Goeppert, A.; Czaun, M.; May, R. B.; Prakash, G. K. S.; Olah, G. A.; Narayanan, S. R., Carbon Dioxide Capture from the Air Using a Polyamine Based Regenerable Solid Adsorbent. *J. Am. Chem. Soc.* **2011,** *133*, 20164-20167.
75. Hiyoshi, N.; Yogo, K.; Yashima, T., Adsorption of Carbon Dioxide on Amine Modified SBA-15 in the Presence of Water Vapor. *Chem. Lett.* **2004,** *33*, 510-511.
76. Knowles, G. P.; Graham, J. V.; Delaney, S. W.; Chaffee, A. L., Aminopropyl-functionalized mesoporous silicas as CO2 adsorbents. *Fuel Process. Technol.* **2005,** *86*, 1435-1448.
77. Knowles, G. P.; Delaney, S. W.; Chaffee, A. L., Diethylenetriamine[propyl(silyl)]-Functionalized (DT) Mesoporous Silicas as CO2 Adsorbents. *Ind. Eng. Chem. Res.* **2006,** *45*, 2626-2633.